Geochemical and isotopic studies of the sedimentary and granitic rocks of the Altai orogen of northwest China and their tectonic implications

BIN CHEN*† & BOR-MING JAHN†

*Department of Geology, Peking University, Beijing 100871, P.R. China
†Université de Rennes 1, Géosciences Rennes (CNRS), Rennes, France

Abstract – The Altai orogen (northwest China) represents the southwestern margin of the Central Asian Orogenic Belt. Geochemical and Nd–Sr isotope analyses were carried out on the Palaeozoic sedimentary and granitic rocks in order to trace their sources and to evaluate the pattern of continental growth of the orogen. Nd isotopic data for both the granites and sediments suggest a significant proportion of middle Proterozoic crust beneath the Altai orogen. However, addition of juvenile material (arc/back-arc oceanic crust) during Palaeozoic times is also significant. Trace elements and isotopic data of sediments suggest their sources were immature. They represent mixtures between a Palaeozoic juvenile component and an evolved continental crust. The early Palaeozoic sediments show $\varepsilon_{Nd}(T) = -3.4$ to -5.0, $T_{DM} = 1.5$–1.8 Ga, and $I_{Sr} = 0.710$–0.712. They represent a passive margin setting, with a predominance of evolved crustal material in the source. The Devonian sequences, however, might have been deposited in a back-arc basin setting, produced by subduction of the Junggar oceanic crust along the Irtysh fault. A significant addition of arc material into the sedimentary basin is responsible for the highly variable ε_{Nd} values (-6 to 0) and I_{Sr} (0.711–0.706). The Carboniferous rocks were also deposited in a back-arc basin setting but with predominantly arc material in the source as suggested by an abrupt increase in $\varepsilon_{Nd}(T)$ ($+6$ to $+3$) and decrease in I_{Sr} (0.7045–0.7051). Voluminous syn-orogenic granitoids have $\varepsilon_{Nd}(T) = +2.1$ to -4.3, $I_{Sr} = 0.705$–0.714 and $T_{DM} = 0.7$–1.6 Ga. They were not derived by melting of local metasedimentary rocks as suggested by previous workers, but by melting of a more juvenile source at depth. Post-orogenic granites have higher $\varepsilon_{Nd}(T)$ ($\sim +4.4$) than the syn-orogenic granitoids, indicating their derivation from a deeper crustal level where juvenile crust may predominate.

1. Introduction

The Altai orogen, extending from Kazakhstan through northern Xinjiang (northwest China) to western Mongolia, represents the southwestern margin of the Central Asian Orogenic Belt. Several models have been proposed to interpret the tectonic evolution of the orogen. Some authors (e.g. Coleman, 1989; Şengör, Natal'in & Burtman, 1993) proposed that the Central Asian Orogenic Belt was developed mainly by accretion of arc complexes, and that the Altai orogen represents a Palaeozoic fold-belt framing the earlier Palaeozoic Sayan-Mogolian fold-belts to the north, possibly interspersed with older continental blocks. Others, however, favoured a process of frequent opening and closing of small oceans that ended with continental collisions, forming the Altai orogen (Xiao *et al.* 1992; Huang, Jiang & Wang, 1992; Zhuang, 1993). This latter model emphasizes the important role of Precambrian crust in the tectonic evolution of the orogen. The old continental crust provided basement for

the deposition of sediments and volcanic rocks, and the emplacement of subduction-related plutons.

The growth of continental crust from a mantle reservoir can be identified from Nd–Sr isotope studies, first of magmatic rocks to constrain the relative contributions of mantle and crustal sources during magma genesis, and second of sedimentary rocks to constrain the average crustal residence age for contributing source regions (Albarede & Brouxel, 1987; Miller & Harris, 1989). Sedimentary rocks usually consist of material derived from various source terranes. The abundance of elements that are relatively insoluble or immobile, such as the rare earth elements (REE), Th and Sc, should reflect the composition of their source area. Therefore, sedimentary rocks will record changes in the chemical and isotopic composition of exposed continental crust and should retain within them a record of new additions of material to the continents. Estimates of the period of residence of sedimentary components within the continental crust are fundamental to investigations of crustal evolution.

Fine-grained sediments are generally assumed to represent the mean composition of a large continental

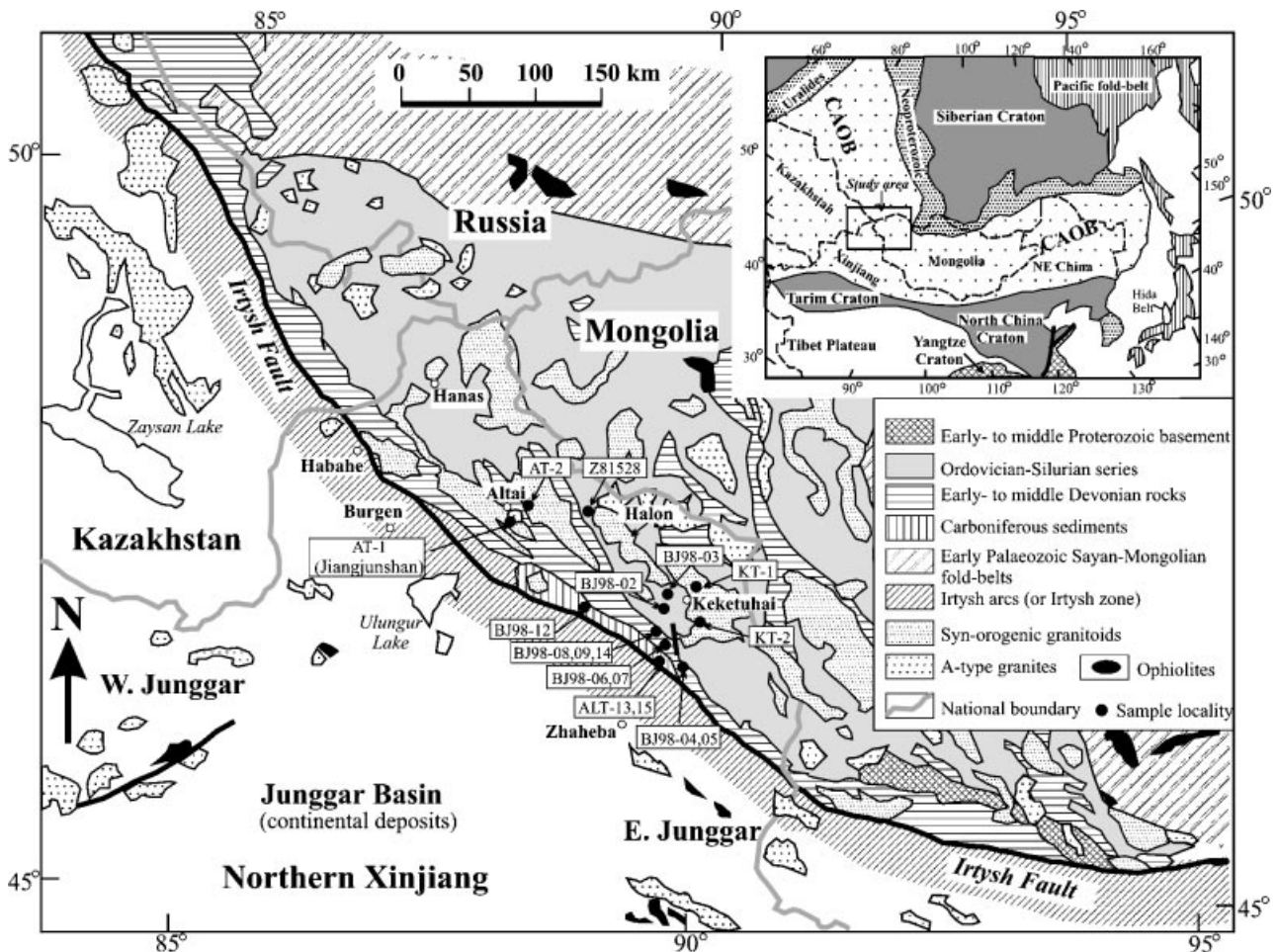* Author for correspondence: bchen@geoms.geo.pku.edu.cn

Figure 1. Geological sketch map of the Altai orogen and neighbouring areas (modified from Chang, Coleman & Ying, 1995). Inset shows simplified tectonic divisions of Asia (modified from Jahn, Wu & Chen, 2000). The Central Asian Orogenic Belt (CAOB) is situated between two major Precambrian cratons: Siberian in the north and North China–Tarim in the south. The Hida Belt of Japan may belong tectonically to the CAOB.

segment (Allegre & Rousseau, 1984; Taylor & McLennan, 1985; Goldstein & Jacobsen, 1988; Jahn & Condie, 1995). The similarity of REE patterns in a variety of fine-grained clastic sedimentary rocks has been taken to imply that little fractionation of Sm/Nd accompanies the generation of clastic sedimentary rocks from their precursors. Consequently, model ages calculated from Sm–Nd data for sedimentary rocks may be expected to reflect the average residence age of the continental portions feeding sedimentary basins (McCulloch & Wasserburg, 1978). Hence, when selecting fine-grained sedimentary rocks covering a range of stratigraphic ages, it is possible to trace back the model age of an eroding continental source and the growth pattern of that continental segment.

In this paper we report the results of a combined Nd–Sr isotope and geochemical investigation of sedimentary and granitic rocks in the Altai orogen. The principal objectives are: (1) to determine the proportion of mantle-derived material versus recycled material that was involved in each continental segment

during each stratigraphic age, and thus to place constraints on the continental growth pattern of this area; (2) to test contrasting petrogenetic models proposed for the granitoids, and to assess the contribution of local metasedimentary rocks in magma genesis.

2. Geological setting and lithological assemblages

The Altai orogen is separated from the Junggar terrane by the NW-trending Irtysh fault (Fig. 1). It consists of NE-facing thrust sheets of Palaeozoic volcano-sedimentary rocks that were deformed and metamorphosed to varying degrees (greenschist to amphibolite facies) by the Caledonian (402–430 Ma, zircon U–Pb: Wang, 1990) and Hercynian (280–330 Ma, zircon U–Pb: Wang, 1990; He *et al.* 1994) orogenies, and intruded by voluminous granitoids (Zhuang, 1993). The lithological assemblages of the Palaeozoic sedimentary rocks are as follows:

(1) Early Palaeozoic (Ordovician–Silurian) sedimentary rocks, comprising essentially terrigenous

clastic and volcaniclastic sedimentary rocks with few volcanic rocks. They were interpreted as passive continental margin sediments by Chang, Coleman & Ying (1995).

(2) Middle Palaeozoic (early and middle Devonian) sequences, deposited unconformably upon the early Palaeozoic sedimentary rocks. They represent a thick marine flysch deposit in which terrigenous clastic rocks, volcano-sedimentary rocks and iron-formations are accompanied by extensive bimodal volcanic rocks (Han & He, 1991; Zhuang, 1993; Yu *et al.* 1993). The lower Devonian sequence is characterized by the occurrence of thick terrigenous clastic rocks in the lower part and rhyolite–latite–dacite sequences with minor interbedded basaltic rocks in the upper part. In contrast, the middle Devonian rocks are bimodal, containing almost equal amounts of acid and submarine basic volcanic rocks, with a marked absence of intermediate rocks. The basic volcanic rocks comprise albite-rich keratophyres and spilitic lavas and tuffs, basaltic pillow lavas (now amphibolites), chert and minor ultramafic rocks, in which polymetallic mineralization (Cu–Pb–Zn–Au) is common. Sedimentary rocks are interbedded with the bimodal volcanic rocks. Rocks of late Devonian age are totally lacking.

(3) Carboniferous sediments comprise marine, fine-grained clastic sediments, with minor volcanic rocks (basaltic and andesitic in composition) and limestone. They were weakly metamorphosed and overthrust the Devonian rocks in middle to late Carboniferous times. However, they were unconformably overlain by Permian continental basin deposits.

Granitic plutons that intrude the Altai orogen are predominantly syn-orogenic granitoids (including typical granites and gneissic equivalents), with minor post-orogenic A-type granites. The syn-orogenic granitoids make up a large part of the orogen (about 40 % by volume). They are undeformed or slightly foliated coarse-grained, porphyritic, biotite/two-mica granitoids; Li-rich and Be-rich variants are locally present. Gradational contacts between the granitic plutons and their host metamorphic rocks indicate their emplacement at a relatively deep crustal level. Emplacement of the granitoids took place at two broad time intervals: late Caledonian (377 to 408 Ma: Zou, Cao & Wu, 1988; Liu, 1990) and Hercynian (290 to 344 Ma: Zou, Cao & Wu, 1988; Liu, 1990; Zhang *et al.* 1996). The late Caledonian granites (e.g. Keketuhai, Halon and Hanas plutons; Fig. 1) are hosted mainly by the early Palaeozoic metasedimentary rocks, whereas the Hercynian granites (e.g. Habahe and Altai plutons) are mainly hosted by middle Palaeozoic rocks (Fig. 1). Recently, a zircon U–Pb (SHRIMP) age of 387 ± 6 Ma (S. A. Wilde, unpub. data) was obtained for the Keketuohai pluton.

The post-orogenic alkaline granites (e.g. Jiangjunshan pluton; Fig. 1) intrude into other lithological units of the Altai orogen and mark the end of the Altai Hercynian orogeny. They are muscovite-rich, and are characterized by the presence of amazonite. Narrow contact-metamorphic aureoles imply emplacement at a high level. The Jiangjunshan pluton has been dated at 151 ± 3 Ma (S. A. Wilde, unpub. data) using SHRIMP methods.

Immediately to the south of the Altai orogen lies the NW-trending Irtysh zone (Fig. 1; Coleman, 1989). This zone is characterized by Devonian to Carboniferous volcanic rocks of andesitic to basaltic composition, and contemporaneous calc-alkaline plutonic rocks (too small to be shown: Mei *et al.* 1993; Yu *et al.* 1993). The rock types are similar to those of the Chenghiz–Tarbgatay volcanic arc in Central Kazakhstan (Coleman, 1989). Thus, the Irtysh zone is thought to represent a middle to late Palaeozoic volcanic arc that is probably associated with subduction of the Junggar oceanic crust beneath the southern margin of the Altai terrane (Mei *et al.* 1993). The Palaeozoic Junggar ocean was first opened in the early Cambrian period, as shown by the evidence of the Tangbale ophiolite with a Pb–Pb age of 523 ± 7 Ma (Kwon, Tilton & Coleman, 1989), and it was not closed until middle Carboniferous times, as indicated by continental deposits that abruptly transgress the earlier Palaeozoic marine facies (Xiao *et al.* 1992; Zhang & Huang 1992).

3. Sample selection and analytical methods

3.a. Sample selection

Sampling of sedimentary rocks was biased towards fine-grained Ordovician, Devonian and Carboniferous clastic rocks. In addition, four representative samples of granites were chosen for chemical and isotopic analyses.

3.b. Analytical methods

Major and trace element abundances were determined by ICP-MS at the Centre de Recherches Petrographiques et Geochimiques (CRPG) in Nancy, France. Analytical uncertainties range from ± 1 % to ± 5 % for major elements; they are approximately ± 5 % for trace elements with abundance ≥ 20 ppm, and approximately ± 10 % for those < 20 ppm (Chen *et al.* 2000).

Nd–Sr isotope analyses were conducted at Géosciences Rennes (CNRS). Sample dissolution was carried out using acid digestion (HNO_3 + HF) in sealed Savillex® beakers on a hot plate (80 °C) for one week; the solution was then dried and the residues re-attacked using acid for two more weeks. Separation of Sm and Nd was done using routine two-column ion-exchange techniques (see Jahn *et al.* 1996; Chen *et al.* 2000 for details). Mass analyses were performed using a seven-collector Finnigan MAT-262 mass spectrometer. $^{87}Sr/^{86}Sr$ ratios were normalized against

$^{86}Sr/^{88}Sr = 0.1194$. The long-term analyses on NBS-987 Sr standard yielded $^{87}Sr/^{86}Sr = 0.710233 \pm 0.000016$ (2σ, 26 analyses) with all ratios adjusted to NBS-987 $^{87}Sr/^{86}Sr = 0.710250$. $^{143}Nd/^{144}Nd$ ratios were normalized against $^{146}Nd/^{144}Nd = 0.7219$. During the period of data acquisition, the Ames internal Nd standard gave $^{143}Nd/^{144}Nd = 0.511967 \pm 0.000002$ (2σ, for 5 analyses) which is equivalent to a La Jolla value of 0.511865. All Nd isotopic ratios reported in Table 2 have been adjusted to La Jolla standard $^{143}Nd/^{144}Nd = 0.511860$.

The uncertainty in concentration measurement by isotope dilution is ± 1–2% for Rb, ± 0.5–1% for Sr, and ± 0.2–0.5% for Sm and Nd depending on concentration levels. The overall uncertainty, including all sources of error, for Rb/Sr is $\pm 2\%$ and Sm/Nd ± 0.2–0.5%. Average procedural blanks are: Sr = 200 pg, Nd = 60 pg. The decay constants used in age calculations are 0.0142 Ga^{-1} for ^{87}Rb and 0.00654 Ga^{-1} for ^{147}Sm. Sm–Nd model ages were calculated based on a depleted mantle (T_{DM}) assuming a linear evolution of isotopic composition from $\varepsilon_{Nd}(T) = 0$ at 4.56 Ga to +10 at the present time.

3.c. Indicators of the source characteristics of metasediments

Some elements such as K, Na, Rb and Sr were probably mobilized during sedimentation and/or metamorphism and thus are of little value in determining the source features of metasediments. Other elements such as REE, Th, Sc and Y, however, are the least fractionated during sedimentation, and are considered to give the best information regarding the sources (Taylor & McLennan, 1985; Jahn & Condie, 1995). Nd isotopes are fairly reliable, due to the immobility of REE. Sr isotopes have only reference value for metasediments, due to their possible open-system behaviour during metamorphism, but they are valuable for granitoids.

4. Results

4.a. Sedimentary rocks

4.a.1. Major and trace elements

Eleven samples of sediments were chosen for chemical analysis (Table 1), and their chemical compositions are shown in Figure 2. Also shown for comparison are middle Proterozoic crust (Zhao *et al.* 1993), post-Archaean average Australian shale (simplified as PAAS in this study; Nance & Taylor, 1976), average arc material (Ewart, 1982) and the Palaeozoic arc rocks from the Irtysh zone (Mei *et al.* 1993). PAAS is considered to be mature, fine-grained clastic sediment and it represents the average composition of the upper continental crust (Nance & Taylor, 1976; Taylor & McLennan, 1985). Arc rocks, however, represent immature material. Therefore, comparison of the Altai sedimentary rocks with the two end-members
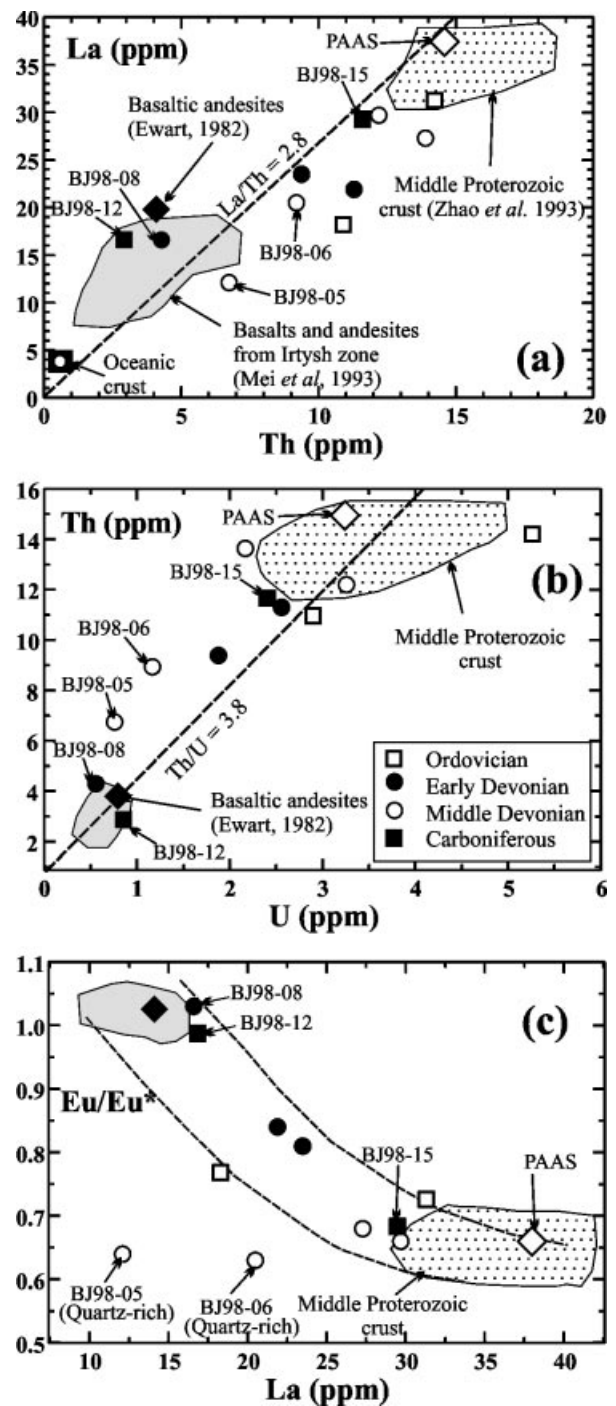
Figure 2. Plots of (a) La vs. Th, (b) Th vs. U and (c) Eu/Eu* vs. La, showing chemical compositions of the Palaeozoic sedimentary rocks. PAAS plots within the field of middle Proterozoic crust in the Altai region, indicating that the latter is also mature. Oceanic crust is from Taylor & McLennan (1985). See text for details.

should be useful for understanding the nature of the eroded continental surface.

The abundances of REE, Th and U, and their ratios (e.g. La/Th, Th/U) provide an index of chemical differentiation. Generally, mature, fine-grained clastic sediments (e.g. loess and post-Archean shales) tend to

Table 1. Chemical compositions of metasedimentary and granitic rocks from the Altai orogen, Xinjiang

Sample no.	BJ98-02	BJ98-03	BJ98-08	BJ98-09	BJ98-14	BJ98-04	BJ98-05	BJ98-06	BJ98-07	BJ98-12	BJ98-15	AT-1	AT-2	KT-1	KT-2
Rock type	Schist	Schist	Schist	Schist	Slate	Qtz-sch.	Qtz-sch.	Qtz-sch.	Schist	Slate	Slate	A-type	Granite	Granite	Granite
Age	Ordov.	Ordov.	D1	D1	D1	D2	D2	D2	D2	Carb.	Carb.	151 Ma	330 Ma	390 Ma	390 Ma
SiO_2 (wt%)	59.32	65.96	64.12	52.98	63.12	77.69	91.51	89.60	61.72	58.35	67.59	78.34	73.69	74.63	72.77
TiO_2	0.84	0.74	0.57	0.97	0.63	0.50	0.12	0.19	0.75	0.84	0.55	0.01	0.08	0.18	0.3
Al_2O_3	18.31	15.46	16.87	21.21	15.28	10.68	3.72	4.94	18.27	18.08	15.65	12.04	14.43	13.44	13.99
FeOt	7.53	6.37	5.88	10.27	6.43	3.22	0.97	1.45	6.36	7.67	3.55	0.57	1.21	2.10	2.39
MnO	0.08	0.07	0.07	0.27	0.08	0.04		0.02	0.06	0.13		0.01	0.03	0.03	0.03
MgO	4.17	3.67	1.78	5.25	2.54	1.53	0.32	0.50	3.53	3.22	0.66	0.01	0.30	0.52	0.56
CaO	1.87	1.08	5.23	1.34	4.03	1.08	0.16	0.50	0.40	2.39	0.26	0.43	0.86	2.38	2.12
Na_2O	2.13	1.08	3.39	2.23	3.82	1.93	0.93	1.38	1.02	3.45	4.03	3.73	3.62	3.02	3.49
K_2O	2.67	2.39	1.32	3.19	1.23	1.79	0.63	0.45	3.54	1.86	3.68	4.09	4.79	2.98	3.48
P_2O_5	0.17	0.16	0.12	0.11	0.14	0.12	0.05	0.05	0.15	0.22	0.08	0.03	0.21	0.06	0.08
LOI	2.81	2.92	0.50	2.10	3.09	1.53	0.68	0.80	4.05	3.71	3.81	0.59	0.58	0.50	0.64
Total	99.90	99.90	99.85	99.92	100.39	100.11	99.09	99.88	99.85	99.92	99.86	99.85	99.80	99.84	99.85
Rb (ppm)	116	74.7	55.6	126	55.2	81.6	36.3	27.3	147	34.0	136	526	217	120	140
Sr	187	116	252	171	389	190	60	114	41	443	146	5.7	74	148	140
Ba	518	638	236	451	210	472	175	100	284	382	593	15	258	543	557
Zr	165	153	187	165	141	206	73.4	101	133	125	163	52.2	72.7	103	183
Nb	10.90	8.45	5.60	9.55	6.46	6.54	1.61	2.53	6.43	4.76	11.0	14.86	8.36	5.99	7.28
Hf	4.4	4.2	4.4	4.1	3.6	5.6	2.1	2.47	3.5	2.9	5.3	4.44	2.5	3.3	5.1
Ta	1.04	0.81	0.31	0.78	0.68	0.66	0.20	0.30	0.69	0.32	0.97	6.69	1.79	0.63	0.83
Th	14.20	10.90	4.29	9.39	11.30	13.90	6.75	9.20	12.20	2.87	11.70	20.30	13.20	15.00	22.3
U	5.28	2.91	0.56	1.88	2.56	2.05	0.76	1.12	3.26	0.88	2.43	1.76	2.75	1.49	2.09
Cs	3.79	1.73	1.92	6.03	0.99	2.48	0.70	0.62	4.80	0.68	4.04	39.10	26.10	8.21	7.9
Y	33.2	26.1	18.1	29.6	22.1	20.1	8.1	10.9	28.4	19.8	23.2	108.9	19.6	36.9	25.1
Pb	26.1	16.1	8.6	13.5	11.4	11.2	7.4	13.3	23.9	9.7	25.1	107.8	37.2	25.3	17.3
V	144.0	114.0	76.1	156.0	116.0	62.6	13.3	17.7	101.0	128.0	56.8	0.6	6.9	21.3	22.3
Cr	160.0	149.0	14.5	175.0	15.8	94.8	19.4	29.6	117.0	58.4	24.6		2.1	6.5	5.5
Co	20.8	17.9	11.1	28.0	14.5	8.4	1.9	3.2	17.1	11.5	9.6	0.1	1.3	3.2	2.85
Ni	98.9	78.0	10.6	125.0	11.3	27.6	7.3	9.3	59.8	22.3	24.4	1.7	2.3	4.0	3.76
Cu	26.0	21.4	13.9	5.4	5.5	13.3	6.2	4.5	65.1	52.3	26.2	1.3	4.0	2.5	2.1
La	31.3	18.2	16.6	23.5	21.9	27.3	12.1	20.5	29.7	17	29.5	6.34	13.69	28.43	36.04
Ce	67.1	38.3	33.5	47.0	43.6	57.1	27.5	38	56.5	39.0	59	14.85	30.02	55.4	70.31
Pr	8.08	5.02	4.09	5.88	5.68	6.75	3.06	4.28	7.18	5.09	7.21	2.22	3.61	7.5	8.22
Nd	31.9	20.2	16.7	22.5	23.0	26.2	10.8	15.3	26.6	19.5	27.8	9.6	12.84	28.42	29.57
Sm	6.81	4.25	3.34	4.36	4.86	4.98	1.96	2.58	5.34	4.64	5.88	4.34	3.11	6.1	5.49
Eu	1.46	1.02	1.11	1.13	1.23	0.996	0.388	0.462	1.05	1.32	1.18	0.04	0.53	1.23	1.21
Gd	5.67	4.01	3.31	4.25	4.23	4.17	1.79	2.03	4.49	3.68	4.97	6.35	3.45	5.89	4.95
Tb	0.918	0.63	0.531	0.638	0.626	0.634	0.232	0.334	0.741	0.536	0.734	1.33	0.56	0.96	0.74
Dy	5.7	3.87	3.18	4.44	3.82	3.5	1.41	1.8	4.54	3.56	4.29	10.58	3.41	5.96	4.3
Ho	1.11	0.836	0.612	0.953	0.794	0.686	0.236	0.358	0.877	0.695	0.776	2.77	0.66	1.3	0.9
Er	3.16	2.35	1.67	2.77	2.22	1.95	0.828	1	2.39	1.93	2.15	8.6	1.74	3.46	2.7
Tm	0.52	0.42	0.256	0.458	0.372	0.315	0.117	0.17	0.397	0.298	0.352	1.58	0.29	0.54	0.43
Yb	3.26	2.48	1.66	3.13	2.4	1.96	0.785	1.04	2.7	1.99	2.33	12.33	1.84	3.69	2.96
Lu	0.508	0.344	0.269	0.491	0.349	0.32	0.133	0.162	0.447	0.298	0.353	2.18	0.35	0.66	0.47
Eu/Eu*	0.73	0.77	1.03	0.81	0.84	0.68	0.64	0.63	0.66	0.99	0.68	0.02	0.50	0.64	0.72
$(La/Yb)_N$	6.3	4.8	6.6	5.0	6.0	9.2	10.2	13.0	7.3	5.6	8.4	0.3	4.9	5.1	8.0
La/Th	2.20	1.67	3.87	2.50	1.94	1.96	1.79	2.23	2.43	5.92	2.52	0.31	1.04	1.90	1.62
Th/U	2.69	3.75	7.66	4.99	4.41	6.78	8.88	8.21	3.74	3.26	4.81	11.53	4.80	10.07	10.67

D1 – early Devonian; D2 – middle Devonian; Ordov. – Ordovician; Carb. – Carboniferous

have higher abundances of La, Th and U, and lower abundances of Co, Sc and Y than their immature counterparts such as greywackes (Taylor & McLennan, 1985; Condie, 1991, 1993; Gallet, Jahn & Torii, 1996). As shown in plots of La–Th (Fig. 2a) and Th–U (Fig. 2b), the sedimentary rocks plot between arc rocks and PAAS (and middle Proterozoic crust) showing abundances of incompatible U, Th and La lower than PAAS, but higher than arc material. This suggests that Th, U and La are inherited from both island arcs and older continental crust. This is further supported by a plot of Eu/Eu*–La (Fig. 2c) in which

most samples (except for the two quartz-rich rocks) fall on a mixing line between arc material and PAAS (and middle Proterozoic crust of the Altai region). Samples BJ98-12 (Carboniferous) and BJ98-08 (early Devonian) plot close to the average basaltic andesites, indicating a predominance of arc material in their sources. Sample BJ98-15 (Carboniferous), however, plots close to the middle Proterozoic crust, though it contains abundant arc components (evidenced by its positive ε_{Nd} value of +3.3; Table 2). This is considered to be ascribed to an extensive fractionation of hornblende (and pyroxene?) and plagioclase during magma
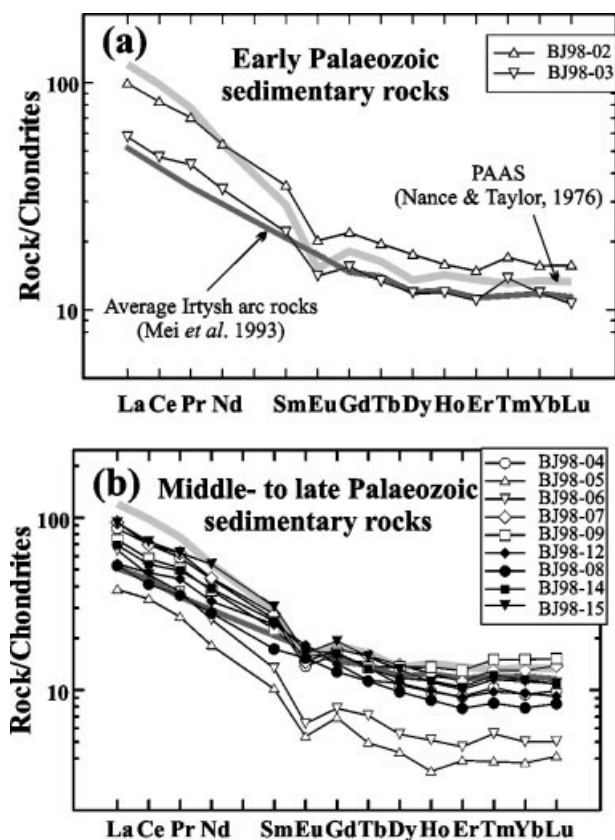
Figure 3. Chondrite-normalized REE patterns of (a) the early Palaeozoic sedimentary rocks and (b) the middle to late Palaeozoic sedimentary rocks. Also shown for comparison are post-Archaean average shales (PAAS; Nance & Taylor, 1976) and average Irtysh arc rocks (Mei *et al.* 1993). Chondrite values: La = 0.315, Ce = 0.813, Nd = 0.595, Sm = 0.193, Eu = 0.0722, Gd = 0.259, Tb = 0.047, Dy = 0.325, Ho = 0.07, Pr = 0.115, Er = 0.213, Tm = 0.0305, Yb = 0.208, Lu = 0.0323. These values are from Masuda, Nakamura & Tanaka (1973), further divided by 1.2 (they choose Leedey chondrites for chemical analysis, which are found to be about 20% higher than the average chondrites.).

evolution of the eroding arc rocks, as is suggested by the low MgO (0.66) and CaO (0.26) and the marked negative Eu anomaly (Eu/Eu* = 0.68; Table 1) of the sample, and probably to accumulation of some accessory phases such as zircon, all of which tends to increase the evolved arc rocks in Th, U and La (Rollinson, 1993, pp. 108–10). Two quartz-rich clastic rocks (BJ98-05, BJ98-06) plot close to the arc field, though they have negative ε_{Nd} values (~ –6.0; Table 2); this is apparently due to the dilution effect of quartz (Fig. 2a,b). Thus, the Altai Palaeozoic sediments are less evolved (more immature) than the old continental crust, and their compositions can be explained by mixing volcanic-arc material and old crust in varying proportions.

Rare earth elements have very low solubility in water and are not significantly fractionated relative to each other during exogenous processes such as

sedimentation and metamorphism; therefore, their abundance and REE patterns should reflect the compositions of their source area (McLennan, 1989; Condie, 1991). The REE patterns are plotted in Figure 3 where they are compared to PAAS and average Irtysh arc rocks (Mei *et al.* 1993). The early Palaeozoic rocks show similar REE patterns to PAAS, with significant negative Eu anomalies (Fig. 3a). This feature suggests a large proportion of mature material in the source region. The middle to late Palaeozoic sedimentary rocks, however, show more complicated patterns (Fig. 3b). Most of them (except for quartz-rich samples BJ98-05 and BJ98-06) show smaller Eu anomalies (Eu/Eu* = 0.68–1.03; Table 1) when compared to PAAS (Eu/Eu* = 0.66; Taylor & McLennan, 1985), suggesting contribution from immature sources (Dickinson *et al.* 1982; Taylor & McLennan, 1985). Samples BJ98-08 and BJ98-12 are distinguished by a total lack of Eu depletion, indicating little contribution from older, mature continental crust, but a significant contribution from island arc sources. Moreover, most samples show LREE patterns transitional between those of basaltic andesites and of PAAS (Fig. 3b), indicating that both volcanic arcs and older continental crust have served as erosional sources (in varying proportions) for the sedimentary rocks.

The quartz-rich clastic rocks (e.g. samples BJ98-05 and BJ98-06), however, show significant negative Eu anomalies (Eu/Eu* = 0.64–0.68) and highly fractionated REE patterns ((La/Yb)$_N$ = 9.2–13). The shapes of the REE patterns are similar to PAAS, although much lower total REE abundances are observed; this is ascribed to the dilution effect of quartz concentration during sedimentary processes.

4.a.2. Nd–Sr isotopes

Nd–Sr isotopic data for eleven sedimentary rocks are given in Table 2 and plotted in Figure 4. The Ordovician–Silurian sediments show negative, slightly varying $\varepsilon_{Nd}(T)$ values (–3.4 to –5.0) with data points close to the field of the Altai middle Proterozoic crust, suggesting that recycled continental crust predominates in the source area. This is supported by their Nd model ages (1.4–1.8 Ga; Table 2), which are much older than their depositional ages (0.46–0.42 Ga), and by their relatively high initial $^{87}Sr/^{86}Sr$ (I_{Sr}) ratios (0.710–0.712; Table 2). Any contribution from juvenile components (e.g. arc material) appears to be minor.

The Devonian sedimentary rocks, however, display a large variation in both $\varepsilon_{Nd}(T)$ values (0 to –6.1) and I_{Sr} ratios (0.706–0.712; Table 2). A different source region from the early Palaeozoic sedimentary rocks is thus indicated for the Devonian rocks. As shown in Figure 4, some data points plot within the middle Proterozoic field. These samples are comparable to the early Palaeozoic (Ordovician–Silurian) sediments, with dominant contribution from old continental

Table 2. Isotopic compositions of sedimentary and granitic rocks from the Altai Mountains, Xinjiang, China

Sample no.	Locality	Age (Ma)	Rock type	Rb (ppm)	Sr (ppm)	$^{87}Rb/^{86}Sr$	$^{87}Sr/^{86}Sr$	2σ	I_{Sr}	Sm (ppm)	Nd (ppm)	$^{147}Sm/^{144}Nd$	$^{143}Nd/^{144}Nd$	2σ	$\varepsilon_{Nd}(0)$	$f_{Sm/Nd}$	$\varepsilon_{Nd}(T)$	T_{DM} (Ga)
BJ98-02	Keketuhai	O (460)	Schist	99.54	195.4	1.474	0.722098	7	0.712438	6.96	33.74	0.1247	0.512221	4	-8.1	-0.37	-3.9	1.59
BJ98-03	Keketuhai	O (460)	Schist	65.59	112.2	1.690	0.721297	7	0.710220	4.36	20.15	0.1307	0.512186	4	-8.8	-0.34	-4.9	1.77
*Z81528	Altai	S (425)	Schist							9.78	50.07	0.1181	0.512245	7	-7.7	-0.40	-3.4	1.44
BJ98-14	Fuyun	D1 (400)	Schist	47.37	382.3	0.358	0.711418	7	0.709376	4.36	20.60	0.1281	0.512436	4	-3.9	-0.35	-0.4	1.27
BJ98-08	Fuyun	D1 (400)	Schist	52.5	274.8	0.552	0.709258	10	0.706111	3.81	17.65	0.1304	0.512465	4	-3.4	-0.34	0.0	1.25
BJ98-09	Fuyun	D1 (400)	Schist	128.3	186.7	1.988	0.720367	8	0.709041	4.75	23.83	0.1205	0.512284	4	-6.9	-0.39	-3.0	1.41
BJ98-04	Fuyun	D2 (385)	Schist	70.61	200.3	1.019	0.716196	7	0.710612	5.26	27.45	0.1159	0.512145	3	-9.6	-0.41	-5.7	1.56
BJ98-05	Fuyun	D2 (385)	Schist	27.10	61.57	1.273	0.718573	7	0.711596	2.10	11.65	0.1090	0.512115	4	-10.2	-0.45	-5.9	1.50
BJ98-06	Fuyun	D2 (385)	Schist	23.05	127.1	0.524	0.714039	8	0.711164	2.87	16.15	0.1073	0.512098	4	-10.5	-0.45	-6.1	1.50
BJ98-07	Fuyun	D2 (385)	Schist	150.6	46.92	9.303	0.743638	7	0.692639	5.75	28.42	0.1223	0.512260	4	-7.4	-0.38	-3.7	1.48
BJ98-12	Altai	C (340)	Slate	36.94	522.8	0.204	0.705484	7	0.704495	5.23	24.64	0.1283	0.512810	4	3.4	-0.35	6.3	0.61
BJ98-15	Altai	C (340)	Slate	115.6	140.0	2.388	0.714631	7	0.705117	5.40	25.97	0.1257	0.512664	4	0.5	-0.36	3.3	0.84
*ALT-15	Fuyun	C (340)	Slate							6.90	33.62	0.1241	0.512627	6	-0.2	-0.37	2.9	0.89
*ALT-13	Fuyun	C (340)	Slate							3.56	16.04	0.1342	0.512680	8	0.8	-0.32	3.5	0.90
(granitoids)																		
AT-1	Altai	151 Ma	A-type	509.9	6.20	259.5	1.652280	13	1.098956	4.31	10.113	0.2576	0.512922	5	5.5	0.31	4.4	0.82#
AT-1	(dupl.)	151 Ma	A-type	508.6	6.15	261.2	1.658548	10	1.101560	3.99	8.909	0.2711	0.512930	4	5.7	0.38	4.3	
AT-2	Altai	330 Ma	Granite	213.7	78.82	7.856	0.740796	7	0.703896	3.42	14.00	0.1476	0.512428	4	-4.1	-0.25	-2.0	1.29#
KT-1	Keketuhai	390 Ma	Granite	115.3	147.4	2.261	0.721709	8	0.709153	6.21	28.06	0.1338	0.512346	3	-5.7	-0.32	-2.6	1.53
KT-2	Keketuhai	390 Ma	Granite	137.1	148.0	2.681	0.721882	8	0.706993	5.62	29.98	0.1133	0.512398	5	-4.7	-0.42	-0.5	1.14
*WQ-12	Keketuhai	390 Ma	Granite	243.6	170.2	4.137	0.727417	28	0.704443	9.27	40.3	0.1391	0.512458	7	-3.5	-0.29	-0.6	1.41
*A81549	Keketuhai	390 Ma	Granite	77.2	86.6	2.575	0.729024	8	0.714724	6.38	26.38	0.1462	0.512425	6	-4.2	-0.26	-1.7	1.63
*JM-18	Halon	390 Ma	Granite	78.48	152.2	1.490	0.716031	7	0.707756	7.85	40.71	0.1166	0.512213	14	-8.3	-0.41	-4.3	1.47
*HL-4	Hanas	390 Ma	Granite	8.29	312.8	0.077	0.70964	29	0.709212	5.37	22.97	0.1413	0.512505	10	-2.6	-0.28	0.1	1.36
*Ha-4	Hanas	390 Ma	Granite	146.6	75.5	5.608	0.744541	11	0.713398	4.19	18.17	0.1394	0.512383	7	-5.0	-0.29	-2.1	1.57
*T-12	Keketuhai	390 Ma	Granite							4.63	22	0.1272	0.512481	11	-3.1	-0.35	0.4	1.18
*DH-5	Halon	390 Ma	Granite							1.97	9.36	0.1272	0.512518	52	-2.3	-0.35	1.1	1.11
*HM-4	Halon	390 Ma	Granite	163.2	101.6	4.643	0.731008	7	0.705224	8.22	37.84	0.1313	0.512500	6	-2.7	-0.33	0.5	1.20
*ALT-20	Altai	330 Ma	Granite	64.77	196.4	0.953	0.712002	17	0.707526	11.18	65.41	0.1033	0.512361	6	-5.4	-0.47	-1.5	1.09
*Tb-5	Altai	330 Ma	Granite	31.15	34.3	2.624	0.723138	30	0.710813	4.44	21.25	0.1263	0.512573	6	-1.3	-0.36	1.7	1.01
*YK-37	Altai	330 Ma	Granite	16.14	268.5	0.174	0.713351	11	0.712534	8.56	49.44	0.1047	0.512387	33	-4.9	-0.47	-1	1.07
*KT-1zh	Keketuhai	330 Ma	Granite	142.5	122.2	3.378	0.723664	8	0.707798	6.46	31.94	0.1223	0.512586	9	-1.0	-0.38	2.1	0.94
*60-4	Altai	330 Ma	Granite	294.9	99.4	8.573	0.737658	10	0.697391	4.31	22.03	0.1183	0.512312	37	-6.4	-0.40	-3.1	1.34
*Hb-4	Habahe	330 Ma	Granite	157.8	122.8	3.714	0.72548	20	0.708035	2.83	30.45	0.0562	0.512434	6	-4.0	-0.71	1.9	0.69
*ALT-18	Altai	330 Ma	Granite	41.6	146.0	0.824	0.715164	8	0.711294	3.38	15.87	0.1287	0.512550	44	-1.7	-0.35	1.1	1.08

(1) $\varepsilon_{Nd} = ((^{143}Nd/^{144}Nd)_s/(^{143}Nd/^{144}Nd)_{CHUR} -1) \times 10000$, $f_{Sm/Nd} = (^{147}Sm/^{144}Nd)_s/(^{147}Sm/^{144}Nd)_{CHUR} -1$, where s = sample, $(^{143}Nd/^{144}Nd)_{CHUR} = 0.512638$ and $(^{147}Sm/^{144}Nd)_{CHUR} = 0.1967$. Model ages ($T_{DM}$) were calculated using an equation assuming a linear growth of Nd isotope ratios: $T_{DM} = 1/\lambda \times \ln(1 + ((^{143}Nd/^{144}Nd)_s - 0.51315)/((^{147}Sm/^{144}Nd)_s - 0.2137))$. Samples with # were calculated using a 2-stage model.

(2) O – Ordovician; S – Silurian; D1 – early Devonian; D2 – mid-Devonian; C – Carboniferous.

(3) Samples with star (*) are from Zhao *et al.* (1993).

crust in the source, as is supported by their old Nd model ages (~ 1.5 Ga). Others, however, fall between the middle Proterozoic and Palaeozoic juvenile crust, strongly suggesting that large amounts of juvenile components were incorporated. Samples BJ98-08 and BJ98-14 have the highest $\varepsilon_{Nd}(T)$ values, indicating involvement of large proportions of arc material in the source. This is consistent with the negligible anomalies of Eu in the REE patterns (Fig. 3b), a feature typical of many arc magmas (Rogers & Hawkesworth, 1989; Sajona *et al.* 1996). Thus, the Nd isotope data coincide with our trace element geochemical data indicating that the sedimentary rocks represent variable mixtures of source rocks, including older continental crust and juvenile arc rocks.

The Carboniferous rocks have higher $\varepsilon_{Nd}(T)$ values (+3.0 to +6.3) and lower I_{Sr} (0.7045–0.7051; Table 2) when compared with the pre-Carboniferous sequences. Correspondingly, they show much younger crustal residence ages (T_{DM}) ranging from 0.6 to 0.9 Ga (Table 2). Figure 4 shows that all the data points fall close to the field of Palaeozoic juvenile

crust, indicating the predominance of juvenile components in the source.

4.b. Granitic rocks

The chemical and isotopic data for granitoids (including both the syn-orogenic and post-orogenic types) are shown in Table 1 and Table 2, respectively. They have relatively high SiO_2 and low FeO, MgO and CaO, and are weakly metaluminous to weakly peraluminous with A/CNK = 0.98–1.08 (Liu, 1990; Zhuang, 1993). On a chondrite-normalized REE plot (Fig. 5a), the syn-orogenic granitoids (excluding the A-type granite) show similar REE patterns: LREE-enriched with flat but relatively high HREE and well-defined negative Eu anomalies. This suggests, when combined with the significant negative anomalies of Ba, Sr, P, Nb and Ti in a primitive mantle-normalized spidergram (Fig. 5b), that the granitoids possess features typical of many crustal melts, with plagioclase, apatite and probably biotite (for depletion of Ba), as main residual phases in the source (Vidal, Cocherie & Le Fort, 1982;
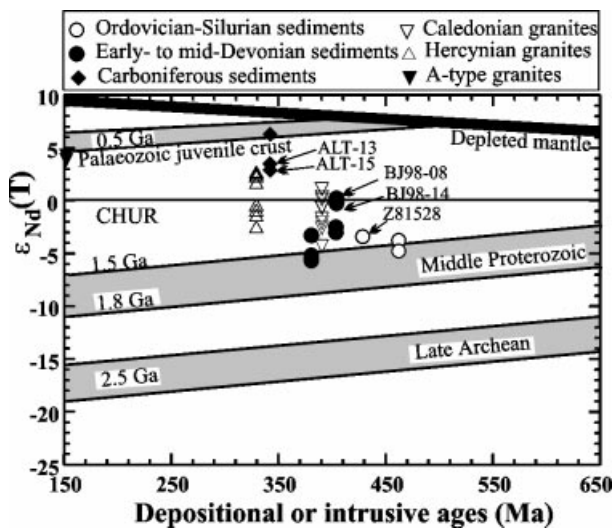
Figure 4. Nd isotopic data for the sedimentary and granitic rocks of the Altai orogen. Epsilon Nd values are calculated for depositional age (sedimentary rocks) or intrusive age (granitic rocks). Data source: Table 2. Three sediment samples ALT-13, ALT-15 and Z81528 are from Zhao *et al.* (1993), but the granite data from Zhao *et al.* (1993) are not marked. See text for details.
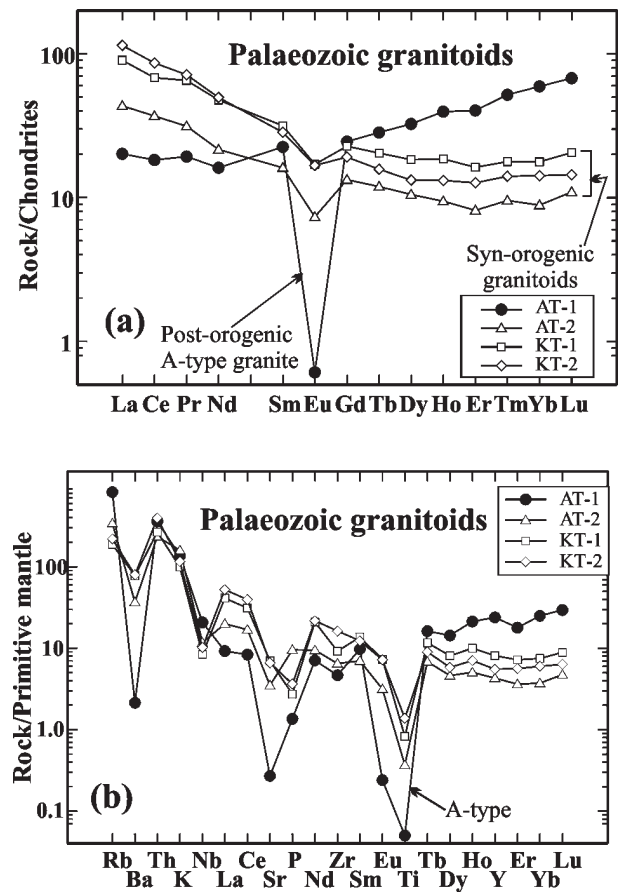

Figure 5. Plots of (a) chondrite-normalized REE patterns of granitoids and (b) primitive mantle (PM)-normalized spidergrams of granitoids. PM values: $TiO_2 = 0.217$, $K_2O = 0.03$, $P_2O_5 = 0.022$, Rb = 0.635, Sr = 21.1, Ba = 6.99, Zr = 11.2, Nb = 0.713, Th = 0.056, Y = 4.55, La = 0.687, Ce = 1.775, Nd = 1.354, Sm = 0.444, Eu = 0.168, Tb = 0.082, Dy = 0.737, Ho = 0.13, Er = 0.48, Yb = 0.493, Lu = 0.074 (Sun & McDonough, 1989). Normalizing values for TiO_2, K_2O, P_2O_5 expressed as wt %; all others in ppm.

Searle & Fryer, 1986). Their crustal origin is also supported by the absence of mafic enclaves within the plutons.

As described previously, published ages for the late Caledonian and Hercynian granitoids vary significantly (Zou, Cao & Wu, 1988; Liu, 1990; Zhang *et al.* 1996). We consider the mean values of 390 Ma and of 330 Ma as the emplacement age of the late Caledonian and Hercynian granitoids, respectively, and initial Nd–Sr isotopic compositions for these granitoids are calculated accordingly. Real intrusive ages may be older or younger than the presumed age by as much as 20 Ma, but this would have little effect on calculated isotopic values (less than 0.2 units, too small to be shown as error bars in Fig. 4). Reported Nd–Sr isotopic data for the Altai granitoids by Zhao *et al.* (1993) were recalculated (see Zhang *et al.* 2001 for analytical details). Figure 4 shows that the $\varepsilon_{Nd}(T)$ values for most granitoids are in the range +2.1 to –4.3. These relatively high but variable $\varepsilon_{Nd}(T)$ values imply involvement of juvenile components in variable proportions in magma genesis. Some plutons such as Keketuhai contain significant proportions of juvenile components as is suggested by their $\varepsilon_{Nd}(T)$ values of around zero (Table 2). However, contribution of crustal material with a long residence time is also significant in some other plutons as indicated by the $\varepsilon_{Nd}(T)$ value of as low as –4.3 (JM-18). Similarly, these granitoids show highly variable I_{Sr} ratios ranging from 0.705 to 0.714 (Table 2), but most of them have comparatively high I_{Sr} (0.708 to 0.710). This is consistent with the

observation in Figure 4 that all data points plot between the fields of Palaeozoic juvenile crust and middle Proterozoic crust. That is, both arc material and old continental crust may have contributed to the generation of the granitoids in the source.

The Jiangjunshan post-orogenic pluton (sample AT-1) shows features typical of A-type granites: huge Eu-depletion and high HREE levels in the REE pattern (Fig. 5a) and pronounced negative anomalies of Ba, Sr, P and Ti in the spidergram (Fig. 5b). Generally, these features are thought to result from significant fractionation of feldspars during magma evolution. Compared to the syn-orogenic granitoids, the A-type granites have even more positive $\varepsilon_{Nd}(T)$ values (+4.4). This is clearly indicated in Figure 4 where the data point plots closer to Palaeozoic juvenile crust, suggesting probable derivation from a deeper crustal level, where juvenile crust predominates.
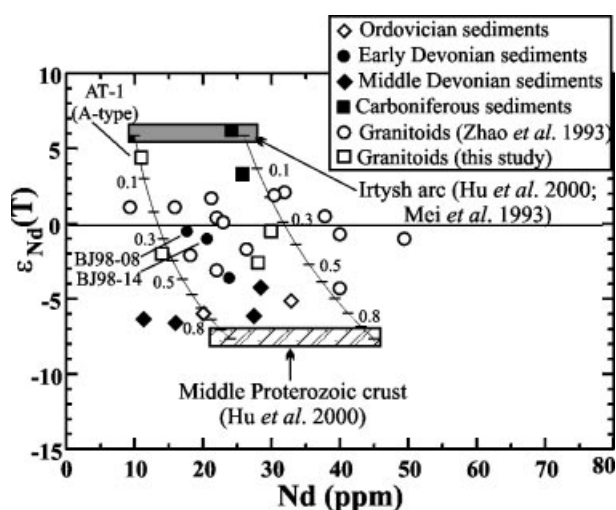
Figure 6. Isotope modelling for a simple mixing in the source region of the sedimentary and granitic rocks. Two end-members are the Irtysh arc rocks, with $\varepsilon_{Nd}(330) = 6.0$ and Nd = 10–26 ppm, and middle Proterozoic crust, with $\varepsilon_{Nd}(330) = -7.5$ and Nd = 24–45 ppm. See text for details.

5. Discussion

5.a. Source regions of sedimentary and granitic rocks

Trace element (including REE) and Nd isotopic data for the sedimentary rocks all indicate that the rocks probably represent variable mixtures of juvenile components and evolved continental crustal material. Possible candidates for the juvenile component are Palaeozoic arc material and/or back-arc oceanic crust, because as previously indicated, an active continental margin setting was produced in the earliest Devonian period, due to N-dipping subduction of the Junggar oceanic crust (Mei *et al.* 1993). Large amounts of arc materials were generated along the Irtysh volcanic zone, and a Devonian back-arc basin was formed, producing significant amounts of back-arc oceanic crust. In addition, substantial involvement of old crustal material is apparent in the sediments, as indicated by the relatively high Nd model ages (mostly T_{DM} = 0.9–1.8 Ga). The T_{DM} values of the sediments suggest a middle Proterozoic basement for the Altai orogen. This idea is further supported by the Nd isotopic data of granitoids that intruded the region.

Figure 6 shows isotopic modelling to constrain the source characteristics of the sediments and granitoids. Nd isotopic data for the two end-members (Irtysh arc and middle Proterozoic crust, with epsilon Nd values of +6.0 and –7.5 at T = 330 Ma, respectively) are from Hu, Jahn & Zhang (2000) and Mei *et al.* (1993). Nd abundances vary significantly (10–26 ppm for the Irtysh arc rocks and 24–45 ppm for the middle Proterozoic crust), due possibly to magmatic evolution. The Ordovician rocks and most middle Devonian rocks contain abundant continental mater-

ial (> 70 %), contrasting to the significant involvement of juvenile (arc) components (~ 50–75 %) in the source of the early Devonian sediments (e.g. BJ98-08 and BJ98-14, consistent with the negligible Eu anomalies of the two samples in Fig. 3b). Two Carboniferous sediments have the highest proportions of arc material (> 85 %).

Granitoids, produced by recycling of continental rocks, are likely to have Sm/Nd ratios not significantly fractionated from their protoliths. Therefore, model ages obtained from young, entirely crust-derived granitoids could be interpreted as reflecting the crustal residence ages of the source rocks. Input of juvenile material derived from a depleted mantle reservoir during magma genesis would raise ε_{Nd} values, hence reducing the resulting model age. Therefore, the model ages of young granites are likely to reflect minimum crustal residence times for the crustal portion of their source region, although the younging effect imparted by the increase in ε_{Nd} values may be partially negated by the probable concurrent increase in the Sm/Nd ratios as a result of mixing a high Sm/Nd mantle component with a low Sm/Nd crustal material (Jahn, Zhou & Li, 1990). Calculated model ages for the granitoids vary from 0.7 Ga to 1.6 Ga (mostly 1.0–1.5 Ga; Table 2); this does not necessarily imply a crust-formation event at that time. Taking into account the large amounts of arc material produced in Palaeozoic times (Şengör, Natal'in & Burtman, 1993), we suggest that the model ages result from mixing of a Palaeozoic arc component with older continental crust which sets a lower limit for the ages of basement rocks in the area. As shown in Figure 4, all granitoid samples plot between a Palaeozoic arc component and middle Proterozoic crust, as in the case of sediments referred to above. Thus, middle Proterozoic crust, together with a juvenile component (Palaeozoic arc and/or back-arc rocks), might have contributed to the generation of the Altai granitoids.

Many Chinese geologists consider the bulk of the Altai granitoids to be typical S-type granitoids derived by melting of the local metasedimentary rocks (e.g. Rui & Wu, 1984; Zhao *et al.* 1993; Zhuang, 1993). This idea is based mainly on the widespread occurrence of mica (particularly muscovite) and presence of gradational contacts with the surrounding metamorphic rocks. Our new isotopic and geochemical data are at variance with this petrogenetic model. Figure 7 compares the isotopic compositions of the sedimentary and granitic rocks, with $\varepsilon_{Nd}(T)$ values for all rocks calculated at T = 330 Ma. The Carboniferous sediments are not included, as the majority of the granitoids were emplaced before or during the deposition of the sediments. As illustrated in Figure 7, the granitoids show significantly higher $\varepsilon_{Nd}(T)$ than the early to middle Palaeozoic (Ordovician, Silurian and Devonian) metasedimentary rocks, although some overlap of data points is evident. Therefore, the local metasedi-
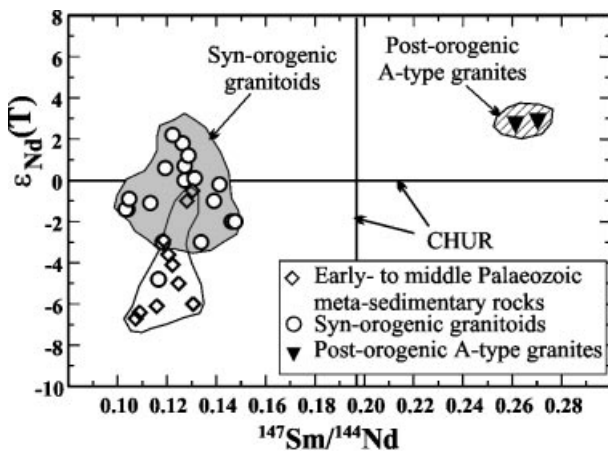
Figure 7. $\varepsilon_{Nd}(T)$ vs. $^{147}Sm/^{144}Nd$ plot of the Palaeozoic sedimentary and granitic rocks of the Altai orogen. The initial Nd isotopic compositions of all samples (including those from Zhao et al. 1993) were calculated at T = 330 Ma.

mentary rocks are unlikely to be the sole source for the granitoids, but could nevertheless have contributed to granitoid generation through contamination. We stress that the granitoids are characterized by relatively high initial ε_{Nd} values (–4.3 to +2.1 (mostly around zero); Fig. 4), indicating a relatively juvenile nature for their source. Thus the Altai granitoids were probably derived from a deeper crustal source, where juvenile (arc) components were abundant (mostly ~ 50–80 % as suggested in Fig. 6). This is in contrast to most European Hercynian granites which are considered to have formed mainly by melting of pre-Hercynian high-grade basement (Bernard-Griffith et al. 1985; Liew & Hofmann, 1988). The juvenile nature of the voluminous granitoids in the Central Asian Orogenic Belt has been well documented in recent years (Şengor, Natal'in & Burtman, 1993; Wickham et al. 1996; Kovalenko et al. 1996; Han et al. 1997; Jahn, Wu & Chen, 2000; Chen et al. 2000), and suggests a significant addition of juvenile continental crust during Phanerozoic times. Our new isotopic data support this model.

5.b. Tectonic implications

Based on our new data, the crustal evolution of the Altai orogen is summarized as follows:

(1) The Nd isotopic compositions ($\varepsilon_{Nd}(T)$ = –3.4 to –5.0) and Nd model ages (1.5–1.8 Ga) calculated for the early Palaeozoic sedimentary rocks clearly indicate that their erosional sources were predominantly re-cycled continental crust (possibly middle Proterozoic) and that little juvenile material was involved. This supports a previous suggestion (Chang, Coleman & Ying, 1995) that the Altai area may have been a passive continental margin during early Palaeozoic times. Field observations also support this model: (1) the early

Palaeozoic rocks are dominated by terrigenous clastic sedimentary rocks with minor volcanism (Zhuang, 1993); and (2) the Junggar ocean, formed in early Cambrian times (Kwon, Tilton & Coleman, 1989; Zhang & Huang, 1992), was characterized by stable sedimentation of limestone and sandstone during the Ordovician and Silurian periods in the northernmost margin (Mei et al. 1993; Yu et al. 1993). The whole early Palaeozoic sequence was deformed and meta-morphosed to varying degrees, and was accreted to the southwestern margin of the Central Asian Orogenic Belt at the end of Silurian times, forming part of the Caledonian orogeny. As a result, the late Caledonian granitoids (377–408 Ma) were emplaced.

(2) Some of the Devonian sediments are character-ized by a marked increase in $\varepsilon_{Nd}(T)$ values and decrease in model ages, clearly indicating a substantial addition of juvenile components in the source com-pared to the early Palaeozoic rocks. These juvenile components came mainly from the Irtysh volcanic arc to the south, in which magmatism of calc-alkaline affinity was extensively developed in the early to mid-dle Devonian period, due to N-directed subduction of the Junggar oceanic crust (Han & He, 1991; Yu et al. 1993; Mei et al. 1993). Therefore, the early Palaeozoic passive continental margin (Altai) might have been converted into an active one in earliest Devonian times. The Devonian sediments were probably deposited in a back-arc basin (marginal sea) that was superimposed upon the previously formed Caledonian fold-belt. This idea is supported by widely developed bimodal volcanism in the early to middle Devonian (Han & He, 1991), consistent with an extensional regime at that time. The voluminous albite-rich keratophyres, basaltic pillow lavas and minor ultramafic rocks produced sug-gest that back-arc spreading might have been extensive enough to create back-arc oceanic crust.

The early to middle Devonian back-arc basin was closed because of convergence of the Tarim and Siberian plates during late Devonian times, consistent with the absence of any late Devonian strata (Zhuang, 1993). Subsequent accretion and crustal thickening result in intense folding, metamorphism (~ 360 Ma; Zhuang, 1993) and emplacement of voluminous gran-itoids at ~ 330 Ma. These events are called the Hercynian orogeny by some workers (Xiao et al. 1992; Zhuang, 1993). The granitoids were derived by partial melting of a middle to lower crustal source that com-prised accreted arc material (or back-arc oceanic crust?) and middle Proterozoic crust. This model is collectively supported by the trace element and Nd isotope tracer study discussed in a previous section.

(3) The Carboniferous sequences were also deposited in a back-arc basin. Both the uplifted Devonian sequence and the newly-formed early Carboniferous volcanic arcs along the Irtysh zone to the south contributed to the sedimentary rocks, caus-ing a significant increase in $\varepsilon_{Nd}(T)$ values (+3.0 to

+6.0). The early Carboniferous volcano-sedimentary rocks were deformed and accreted to the southern margin of the Altai Hercynian orogen during middle to late Carboniferous times, as a result of the convergence and collision of the Siberian and Tarim cratons (Xiao *et al.* 1992).

The post-orogenic granites intruded into the Altai orogen after cessation of regional compression, with the onset of relaxation and extension. They represent the final tectono-magmatic event in the Palaeozoic orogen of this region. The isotopic signature of the alkaline granites indicates that the lower crust in the Altai area is dominated by relatively young continental material, which is possibly the arc material and back-arc oceanic crust buried by subsequent volcano-sedimentary deposits. It is commonly accepted that mantle-derived magma may become available to underplate newly consolidated crust, which in turn triggers the partial melting of the lower crust, resulting in the formation of high-temperature dry granitic melts (Bergantz, 1989; Azevedo & Nolan, 1998).

6. Conclusions

Our data allow the following conclusions to be made:

(1) Nd isotope analyses of Palaeozoic sedimentary and granitic rocks reveal a middle Proterozoic basement beneath the Altai orogen, and a significant addition of 'juvenile' continental crust during Palaeozoic times.

(2) The Altai Palaeozoic sedimentary rocks are less differentiated and more immature than post-Archaean average shales (PAAS). They represent variable mixtures of Palaeozoic arc material/back-arc oceanic crust and middle Proterozoic continental crust. The voluminous syn-orogenic granitoids were not derived from melting of local metasedimentary rocks (although contamination by them is possible), but from melting of a relatively juvenile source at depth, where Palaeozoic arc material (or back-arc oceanic crust?) is abundant. The post-orogenic granites (A-type) show even higher $\varepsilon_{Nd}(T)$ values than the syn-orogenic granites, indicating their derivation from a source where back-arc oceanic crust/arc material may predominate.

(3) The development of the Altai orogen was closely associated with the formation and evolution of the Palaeozoic Junggar ocean lying to the south. The early Palaeozoic sequences represent a passive continental margin setting. However, an active continental margin environment (back-arc basin/marginal sea) developed in the early to middle Devonian, due to the onset of N-directed subduction of Junggar oceanic crust. This is indicated by an extensive development of bimodal volcanism and by a significant increase of $\varepsilon_{Nd}(T)$ values for some of the sedimentary rocks.

References

ALBAREDE, F. & BROUXEL, M. 1987. The Sm/Nd secular evolution of the continental crust and the depleted mantle. *Earth and Planetary Science Letters* **82**, 25–35.

ALLEGRE, C. J. & ROUSSEAU, D. 1984. The growth of the continent through geological time studied by Nd isotope analysis of shales. *Earth and Planetary Science Letters* **67**, 19–34.

AZEVEDO, M. R. & NOLAN, J. 1998. Hercynian late-post-tectonic granitic rocks from the Fornos de Algodres area (Northern Central Portugal). *Lithos* **44**, 1–20.

BERGANTZ, G. W. 1989. Underplating and partial melting: implications for melt generation and extraction. *Science* **245**, 1093–5.

BERNARD-GRIFFITH, J., PEUCAT, J. J., SHEPPART, S. & VIDAL, P. 1985. Petrogenesis of Hercynian leucogranites from the southern Armorican Massif: contribution of REE and isotopic (Sr, Nd, Pb and O) geochemical data to the study of source rock characteristics and ages. *Earth and Planetary Science Letters* **74**, 235–50.

CHANG, E. Z., COLEMAN, R. G. & YING, D. X. 1995. *Tectonic Transect Map across Russia–Mongolia–China.* Stanford University Press.

CHEN, B., JAHN, B. M., WILDE, S. & XU, B. 2000. Two contrasting Palaeozoic magmatic belts in northern Inner Mongolia, China: petrogenesis and tectonic implications. *Tectonophysics* **328**, 157–82.

COLEMAN, R. G. 1989. Continental growth of Northwest China. *Tectonics* **8**, 621–35.

CONDIE, K. C. 1991. Another look at REE in shales. *Geochimica et Cosmochimica Acta* **5**, 2527–31.

CONDIE, K. C. 1993. Chemical composition and evolution of the upper continental crust – contrasting results from surface samples and shales. *Chemical Geology* **104**, 1–37.

DICKINSON, W. R., INGERSOLL, R. V., COWAN, D. S., HELMOLD, K. P. & SUCZEK, C. A. 1982. Provenance of Franciscan greywackes in coastal California. *Geological Society of America Bulletin* **93**, 95–107.

EWART, A. 1982. The mineralogy and petrology of Tertiary–Recent orogenic volcanic rocks: with special reference to the andesitic–basaltic compositional range. In *Andesites: orogenic andesite and related rocks* (ed. R. S. Thorpe), pp. 25–95. Wiley.

GALLET, S., JAHN, B. M. & TORII, M. 1996. Geochemical characterization of the Luochuan loess–paleosol sequence, China, and paleoclimatic implications. *Chemical Geology* **133**, 67–88.

GOLDSTEIN, S. J. & JACOBSEN, S. B. 1988. Nd and Sr isotopic systematics of river suspended material: implications for crustal evolution. *Earth and Planetary Science Letters* **87**, 249–65.

HAN, B. F. & HE, G. Q. 1991. The tectonic nature of the

Devonian volcanic belt of the southern margin of Altai Mountains, China. *Geoscience of Xinjiang* no. 3, 89–100 (in Chinese).

HAN, B. F., WANG, S. G., JAHN, B. M., HONG, D. W., KAGAMI, H. & SUN, Y. L. 1997. Depleted-mantle magma source for the Ulungur River A-type granites from north Xinjiang, China: geochemistry and Nd–Sr isotopic evidence, and implication for Phanerozoic crustal growth. *Chemical Geology* **138**, 135–59.

HE, G. Q., LI, M. S., LIU, D. Q., TANG, Y. L. & ZHOU, R. H. 1994. *Palaeozoic Crustal Evolution and Mineralization in Xinjiang, China*, pp. 71–3. Hong Kong: Educational and Cultural Press Ltd. (in Chinese with English abstract)

HU, A. Q., JAHN, B. M. & ZHANG, Y. 2000. Crustal evolution and Phanerozoic crustal growth in northern Xinjiang: Nd isotopic evidence. Part I. Isotopic characterization of basement rocks. *Tectonophysics* **328**, 15–52.

HUANG, T. K., JIANG, C. & WANG, Z. 1992. On the accordion movement of plate tectonics of Xinjiang and neighbouring areas. In *Tectonics in northern Xinjiang and its neighbouring areas*, pp. 3–13. Beijing: Geological Publishing House (in Chinese).

JAHN, B. M. & CONDIE, K. C. 1995. Evolution of the Kaapvaal craton as viewed from geochemical and Sm–Nd isotopic analyses of intracratonic pelites. *Geochimica et Cosmochimica Acta* **59**, 2239–58.

JAHN, B. M., CORNICHET, J., CONG, B. L. & YUI, T. F. 1996. Ultrahigh-ε_{Nd}(T) eclogites from an ultrahigh pressure metamorphic terrane of China. *Chemical Geology* **127**, 61–79.

JAHN, B. M., WU, F. Y. & CHEN, B. 2000. Massive granitoids generation in Central Asia: Nd isotope evidence and implication for continental growth in the Phanerozoic. *Episodes* **23**, 82–92.

JAHN, B. M., ZHOU, X. H. & LI, J. L. 1990. Formation and tectonic evolution of Southeastern China and Taiwan: isotopic and geochemical constraints. *Tectonophysics* **183**, 145–60.

KOVALENKO, V. I., YARMOLYUK, V. V., KOVACH, V. P., KOTOV, A. B., KOZAKOV, I K. & SAL'NIKOVA, E. B. 1996. Sources of Phanerozoic granitoids in Central Asia: Sm–Nd isotope data. *Geochemistry International* **34**, 628–40.

KWON, S. T., TILTON, G. R. & COLEMAN, R. G. 1989. Isotopic studies bearing on the tectonics of the West Junggar region, Xinjiang, China. *Tectonics* **8**, 719–27.

LIEW, T. C. & HOFMANN, A. W. 1988. Precambrian crustal components, plutonic associations, plate environment of the Hercynian Fold Belt of central Europe: indications from a Nd and Sr isotopic study. *Contributions to Mineralogy and Petrology* **98**, 129–38.

LIU, W. 1990. Ages and petrogenesis of granitoids in the Altai Mts., Xinjiang, China. *Geotectonica et Metallogenia* **14**, 43–56 (in Chinese with English abstract).

MASUDA, A., NAKAMURA, N. & TANAKA, T. 1973. Fine structures of mutually normalized rare earth patterns of chondrites. *Geochimica et Cosmochimica Acta* **37**, 239–48.

MCCULLOCH, M. T. & WASSERBURG, G. J. 1978. Sm–Nd and Rb–Sr chronology of continental crust formation. *Science* **200**, 1003.

MCLENNAN, S. M. 1989. Rare earth elements in sedimentary rocks: influence of provenance and sedimentary processes. In *Geochemistry and Mineralogy of Rare Earth Elements* (eds B. R. Lipin and G. A. McKay), pp. 169–200. Mineral Society of America, Washington, D. C.

MEI, H. J., YANG, X. C., WANG, J. D., YU, X. Y., LIU, T. G. & BAI, Z. H. 1993. Trace element geochemistry of late Palaeozoic volcanic rocks on the southern side of the Irtysh River and the evolutional history of tectonic setting. In *Progress of solid-earth sciences in northern Xinjiang, China* (ed. G. Z. Tu), pp. 199–216. Beijing: Science Press (in Chinese).

MILLER, J. F. & HARRIS, N. B. W. 1989. Evolution of continental crust in the Central Andes: constraints from Nd isotope systematics. *Geology* **17**, 615–17.

NANCE, W. B. & TAYLOR, S. R. 1976. Rare earth element patterns and crustal evolution – I. Australian post-Archean sedimentary rocks. *Geochimica et Cosmochimica Acta* **40**, 1539.

ROGERS, G. & HAWKESWORTH, C. J. 1989. A geochemical traverse across the North Chilean Andes: evidence for crust generation from the mantle wedge. *Earth and Planetary Science Letters* **91**, 271–85.

ROLLINSON, H. 1993. *Using Geochemical Data: evolution, presentation, interpretation*. Essex: Longman.

RUI, X. J. & WU, Y. J. 1984. Petrogenesis of the granitoids in Altai, China. In *Granite Geology and its Relation to Metallogeny* (ed. K. Q. Xu), pp. 14–21. Nanjing: Jiangsu Science and Technology Press (in Chinese with English abstract).

SAJONA, F., MAURY, R. C., BELLON, H., COTTON, J. & DEFANT, M. 1996. High field strength element enrichment of Pliocene–Pleistocene island-arc basalts, Zamboanga Peninsula, Western Mindanao (Philippines). *Journal of Petrology* **37**, 693–726.

SEARLE, M. P. & FRYER, B. J. 1986. Garnet-, tourmaline- and muscovite-bearing leucogranites, gneisses and migmatites of the higher Himalayas from Zanskar, Kulu, Lahoul and Kashmir. In *Collision Tectonics* (eds M. P. Coward and A. C. Ries), pp. 185–202. Geological Society of London, Special Publication no. 19.

ȘENGÖR, A. M. C., NATAL'IN, B. A. & BURTMAN, V. S. 1993. Evolution of the Altaid tectonic collage and Palaeozoic crustal growth in Eurasia. *Nature* **364**, 299–307.

SUN, S. S. & MCDONOUGH, W. E. 1989. Chemical and isotopic systematics of oceanic basalts: implications for mantle composition and processes. In *Magmatism in the Ocean Basins* (eds A. D. Saunders and M. J. Norry), pp. 313–45. Geological Society of London, Special Publication no. 42.

TAYLOR, S. R. & MCLENNAN, S. M. 1985. *The Continental Crust: Its Composition and Evolution*. Oxford: Geoscience Texts, Blackwell.

VIDAL, P., COCHERIE, A. & LE FORT, P. 1982. Geochemical investigations of the origin of the Manaslu leucogranite (Himalaya, Nepal). *Geochimica et Cosmochimica Acta* **46**, 2279–92.

WANG, Z. G. 1990. Petrogenesis of the granitoids of the Altai Orogen. *Geoscience of Xinjiang*, no. 1, 69–77 (in Chinese with English abstract).

WICKHAM, S. M., ALBERT, A. D., ZANVILEVICH, A. N., LITVINOVSKY, B. A., BINDEMAN, I. N. & SCHUBLE, E. A. 1996. A stable isotope study of anorogenic magmatism in East Central Asia. *Journal of Petrology* **37**, 1063–95.

XIAO, X. C., TANG, Y. Q., FENG, Y., ZHU, B., LI, J. & ZHOU, M. 1992. *Tectonics in northern Xinjiang and its neighbouring areas*, pp. 104–21. Beijing: Geological Publishing House (in Chinese with English abstract).

YU, X. Y., MEI, H. J., YANG, X. C. & WANG, J. D. 1993. Irtysh volcanic rocks and tectonic evolution. In *Progress of solid-earth sciences in northern Xinjiang, China* (ed. G. Z. Tu), pp. 185–98. Beijing: Science Press (in Chinese with English abstract).

ZHANG, Q. & HUANG, X. 1992. Age and tectonic setting of the ophiolite in W. Junggar, Xinjiang. *Geological Review* **38**, 509–22 (in Chinese with English abstract).

ZHANG, X. B., SUI, J. X., LI, Z. & LIU, W. 1996. *Tectonic Evolution of the Irtysh Zone and Metallogenesis*, pp. 89–91. Beijing: Science Press.

ZHAO, Z. H., WANG, Z. G., ZOU, T. R. & MASUDA, A. 1993. The REE, isotopic composition of O, Pb, Sr and Nd and petrogenesis of granitoids in the Altai region. In *Progress of solid-earth sciences in northern Xinjiang, China* (ed. G. Z. Tu), pp. 239–66. Beijing: Science Press (in Chinese with English abstract).

ZHUANG, Y. X. 1993. *Tectonothermal Evolution in Space and Time and Orogenic Processes of the Altaide, China*. Changchun: Jilin Science and Technology Press, pp. 10–60 (in Chinese with English abstract).

ZHANG, Y. Q., XIE, Y. W., LI, X. H., QIU, H. N. & ZHAO, Z. H. 2001. Isotopic characteristics of shoshonitic rocks in eastern Qinhai–Tibet Plateau: Petrogenesis and its tectonic implication. *Science in China (Ser. D)* **44**, 1–6.

ZOU, T. R., CAO, H. Z. & WU, B. Q. 1988. Discrimination of orogenic- and anorogenic granites in Altai, Xinjiang. *Acta Geologica Sinica* **3**, 228–43 (in Chinese with English abstract).